Unlocking the Potential of Papuan Red Fruit (*Pandanus conoideus* Lam): A Comprehensive Exploration of Its Role in COVID-19 Inhibition Through Molecular Docking and Molecular Dynamics Simulation

Agus Dwi Ananto[1,2], Harno Dwi Pranowo[1*], Winarto Haryadi[1], and Niko Prasetyo[1]

[1]*Department of Chemistry, Faculty of Mathematics and Natural Sciences, Universitas Gadjah Mada, Sekip Utara, Yogyakarta 55281, Indonesia*

[2]*Department of Pharmacy, Faculty of Medicine and Health Science, Universitas Mataram, Jl. Majapahit No. 62, Mataram 83115, Indonesia*

* ***Corresponding author:***

email: harnodp@ugm.ac.id

Received: August 28, 2024
Accepted: February 5, 2025

DOI: 10.22146/ijc.99486

Abstract: *Indonesia's rich flora has long been used in traditional herbal medicine, and scientific research is now confirming the health benefits of these plants. Among them, Papuan Red Fruit is gaining attention for its potential in treating various ailments, including COVID-19, due to its antioxidant and antibacterial properties. This study focuses on using* in silico *methods to investigate how Papuan Red Fruit might inhibit COVID-19, specifically by targeting the papain-like protease (PLpro), a key protein in viral replication. Molecular docking and molecular dynamics (MD) simulations were used to assess the binding affinity and stability of compounds from the fruit. The compound quercetin 3'-glucoside showed the lowest binding energy, indicating strong interactions with PLpro. MD simulations at 300 K for 100 ns confirmed the stability of the quercetin 3'-glucoside-PLpro complex, revealing hydrogen bonds with residues like GLN169. The simulations showed an average delta RMSD of 0.2702 Å, indicating the complex's stability. Overall, this research highlights the potential of Papuan Red Fruit as a natural treatment for COVID-19, opening the door for further studies in drug development.*

Keywords: *Papuan Red Fruit; molecular docking; MD simulation; SARS-CoV-2 PLpro*

■ INTRODUCTION

Using Indonesia's distinctive flora as an herbal plant represents a rich tradition deeply rooted in the country's cultural and medicinal heritage. These herbal plants have been passed down through generations, with indigenous communities harnessing their healing potential for various ailments. Moreover, Indonesia's herbal plants are gaining recognition beyond its borders with increasing global interest in natural remedies and alternative medicine. Scientific studies continue to unveil the pharmacological benefits of these plants, reinforcing their status as invaluable resources for holistic health. As Indonesia moves forward, the sustainable cultivation and preservation of these botanical treasures remain paramount, ensuring that future generations can continue to benefit from the therapeutic wonders of Indonesia's herbal legacy [1-3].

Red Fruit is one of the Indonesian plants that holds potential as an herbal medicine. Papuan Red Fruit, indigenous to the lush landscapes of Papua, Indonesia, stands as a beacon of natural potency and healing. Renowned for its vibrant hue and rich nutritional profile, this exotic fruit has captivated locals and researchers for its potential therapeutic properties. Bursting with antioxidants [4-5], antiseptic [6], anticancer [7], anti-diabetic peripheral neuropathy agent [8], immunomodulator [9], and antibacterial [10]. Papuan Red Fruit emerges as a promising candidate in the fight against various ailments, including its recent exploration into combatting COVID-19.

Globally, JN.1 stands out as the most frequently reported Variant of Interest (VOI), now identified in 115 countries, comprising 90.3% of sequences in week nine, a slight increase from 89.4% in week six. Conversely, its precursor lineage, BA.2.86, has declined, representing 2.2% of sequences in week nine compared to 3.0% in week six. Over the past 28-day period from 5 February to 3 March 2024, there has been a significant 44% reduction in the number of new COVID-19 cases compared to the preceding 28-day period from 8 January to 4 February 2024, with over 292,000 new cases recorded globally. Similarly, there has been a notable 51% decrease in new deaths during this period, with 6,200 fatalities reported. As of 3 March 2024, the global tally has over 774 million confirmed cases and more than 7 million deaths. Additionally, from 5 February to 3 March 2024, new hospitalizations and admissions to intensive care units (ICUs) have decreased overall, with reductions of 35% and 64%, totaling over 78,000 hospitalizations and 500 ICU admissions [11].

To combat the COVID-19 pandemic, research is diligently directed towards identifying inhibition targets within the virus, notably focusing on non-structural proteins such as papain-like protease (PLpro). PLpro, a crucial enzyme in the replication cycle of coronaviruses, plays a pivotal role in processing viral proteins necessary for replication and dissemination. Thus, inhibition of PLpro presents a promising strategy for impeding the virus's development and spread. Various studies and clinical trials are underway to pinpoint compounds or drugs capable of inhibiting PLpro activity and to develop effective and safe therapies to combat COVID-19.

The research by Kandeel et al. [12] explores the repurposing potential of FDA-approved drugs against the PLpro of SARS-CoV-2, aiming to identify existing compounds that could effectively inhibit viral replication. Through molecular docking simulations, the study investigates the binding affinities of various antivirals, antibiotics, anthelmintics, antioxidants, and cell protectives to the PLpro enzyme. The findings reveal several promising candidates with high binding scores, suggesting their potential as inhibitors of PLpro activity [12]. Other research by Pang et al. [13] delves into the quest for a small molecule inhibitor capable of targeting the PLpro associated with COVID-19. Employing a multifaceted approach, they utilize structure-based virtual screening, molecular dynamics (MD) simulation, and molecular mechanics/generalized Born surface area (MM/GBSA) calculation to sift through vast molecular databases in search of potential inhibitors. Their meticulous methodology yields promising results, culminating in successfully identifying a candidate small molecule inhibitor with notable efficacy against PLpro [13]. These findings underscore the importance of computational techniques in drug discovery and provide a solid foundation for future research endeavors to develop novel therapeutic interventions to combat COVID-19.

Previous studies have shown that flavonoid compounds, particularly quercetin, have the potential to inhibit PLpro of SARS-CoV-2 through both *in silico* and *in vitro* approaches. Rizzuti et al. [14] reported the effectiveness of quercetin in inhibiting the main protease (3CLpro) of SARS-CoV, strengthening the idea that flavonoids can serve as promising antiviral agents. Another study by Kashyap et al. [15] utilized molecular docking to identify quercetin as one of the compounds capable of effectively binding to the active site of PLpro SARS-CoV-2, showing strong protein-ligand interactions. These studies not only highlight the relevance of quercetin and its derivatives as therapeutic candidates but also emphasize the efficiency and precision of *in silico* methods in identifying new compounds for antiviral development, particularly those targeting PLpro of SARS-CoV-2.

Molecular docking is a well-established computational technique employed in drug discovery, offering insights into ligand-target interactions and structure-activity relationships (SAR) without prior knowledge of the chemical structure of potential target modulators [16]. This approach enables scientists to assess the effectiveness against COVID-19 by evaluating the binding energy of a compound and gauging its capacity to bind to the receptor and interact with specific amino acid residues through a specialized bond type [17]. Through the examination of bodily system

dynamics, MD simulations can unveil the stability complex of the ligand-protein interaction [18-19]

The authors believe that targeting the PLpro of COVID-19 remains highly relevant as a virus inhibition strategy despite its numerous mutations. Through deep investigation utilizing sophisticated techniques such as molecular docking, and MD simulation, this study aims to unveil the molecular secrets behind the remarkable ability of Papuan Red Fruit to inhibit the development of the Mpro of COVID-19 virus. With each stride in research, the allure of Papuan Red Fruit as a natural remedy continues to burgeon, offering hope and resilience in the face of global health challenges.

■ EXPERIMENTAL SECTION

Materials

The hardware used is a computer equipped with a 13th Gen Intel i7-13700KF CPU running at 5.3 GHz, 64 GB RAM with an Ubuntu 22.04.3 LTS x86_64 operating system, and an RTX Nvidia GPU. The primary software installed is Yasara-Structure 23.8.19 [20] and Discovery Studio Visualizer (DSV) 21.1.0.20298 [21]. All software settings were left at their default values.

Procedure

The structural data for SARS-CoV-2 PLpro (PDB ID: 7JIR) was obtained from the Protein Data Bank [20,22]. This structure underwent preparation, including removing water molecules and ions using Yasara-structure tools. While the native ligand, 5-amino-2-methyl-*N*-[(1*R*)-1-naphthalen-1-ylethyl]benzamide (TTT), remained for benchmarking the potential of herbal bioactive compounds as competitors. To validate the docking methodology, redocking with 25 iterations of the native ligand was conducted utilizing the Yasara-structure. Preparation initiates with the separation of the protein from its native ligand. Subsequently, all alterations to compound configurations undergo energy minimization before advancing to the molecular docking phase.

Molecular docking

The docking method utilized to calculate the binding energy value is based on Yasara-structure, employing a force field AMBER scoring function approach. A simulation box with a radius of 5.0 Å was created around the outermost part of the native ligand to facilitate the docking process. Binding energy calculations were performed using the Vina docking method integrated within Yasara-structure, and the receptor residues engaged in the interaction were identified. Upon completion of the docking process, the results were saved in the PDB (.pdb) file format. Subsequently, the post-docking data underwent analysis and visualization using DSV. Papuan Red Fruit, scientifically known as *Pandanus conoideus* Lam, is notable for its carotenoid and flavonoid content, as detailed in Table 1 [23-24]. The docking process was conducted for this fruit's carotenoid and flavonoid compounds.

MD simulation

MD simulation was conducted to evaluate the structural stability of the top compounds identified from prior molecular docking studies. The MD simulation using Yasara-structure encompassed preparation, minimization, equilibration, and production phases. During the preparation phase, essential parameters included a cubic simulation cell containing water solvents, periodic boundary conditions, a membrane box sized 30 Å larger than the protein, and a water box sized 20 Å larger than the protein. Additionally, the simulation incorporated 0.9% NaCl ions, utilizing the AMBER14 force field. The conditions were set to a pH of 7.4, a temperature of 300 K, and a pressure of 1 bar [25-26]. Running at a time step of 2.5 fs, the simulation data were automatically saved in .sim file format throughout 100 ns. Post-simulation, the md_analyze.mcr macro command in Yasara-structure was used to determine root-mean-square-deviation (RMSD) values.

■ RESULTS AND DISCUSSION

Molecular Docking

Molecular docking is a powerful computational technique that can accurately predict the structure of ligand-protein complexes. Docking studies provide valuable insights into how the drug binds to the protein by simulating the interaction between a drug candidate

and its target protein [27]. This information is crucial for understanding the potential affinity and activity of the drug, which are vital factors in its efficacy and therapeutic potential. Through these simulations, researchers can visualize the binding sites, orientations, and interactions at the molecular level, optimizing drug design and the development of more effective treatments. As a result of the docking simulation, the docking score is employed to measure the binding energy value. This score reflects the strength of the ligand and receptor interaction, providing a quantitative assessment of their binding affinity. By evaluating this interaction, researchers can gain insights into the stability and efficacy of the ligand-receptor complex, which is essential for advancing drug development and optimizing therapeutic strategies [28].

For several reasons, SARS-CoV-2 PLpro is considered a potential target for COVID-19 inhibition. PLpro is crucial for the virus's life cycle as it processes the viral polyprotein into functional units necessary for viral replication. This protease also modulates the host's immune response by cleaving ubiquitin and ISG15 from host proteins, which helps the virus evade the host's antiviral mechanisms [22,29]. Inhibiting PLpro can hinder the virus's ability to replicate and simultaneously restore the host's immune response. Structural studies, including those involving the mutant form of PLpro in complex with inhibitors, provide detailed insights into how inhibitors can bind to and inhibit this protease [24,30]. The combination of its essential role in viral replication and immune evasion, along with detailed structural data, supports the potential of SARS-CoV-2 PLpro as a target for therapeutic intervention in COVID-19.

The Yasara-structure software was utilized to separate the native ligand from the protein, yielding the native ligand data (7jir_ligand.yob) and the protein (7jir_receptor.sce). The molecular docking method was then validated through 100 re-docking iterations using the native ligand, following the procedure outlined by Ananto et al. [31]. The results demonstrated an average RMSD value of 0.228 Å (Fig. 1), confirming the validity of the molecular docking method employed. Notably, an RMSD value below 2 Å serves as a critical indicator, affirming the robustness and viability of the employed docking protocol. This value signifies the accuracy and reliability of the computational approach in predicting ligand binding orientations within the target protein structure.

After confirming the validity of the docking method, all flavonoid and carotenoid derivatives found in Red Fruit was subjected to docking procedures. Additionally, we included remdesivir and paxlovid as reference compounds for comparative analysis. The docking results of these compounds are presented in Table 1.

Based on the docking results, it is evident that quercetin 3'-glucoside exhibits the lowest binding energy among the tested compounds (−8.244 kcal/mol).

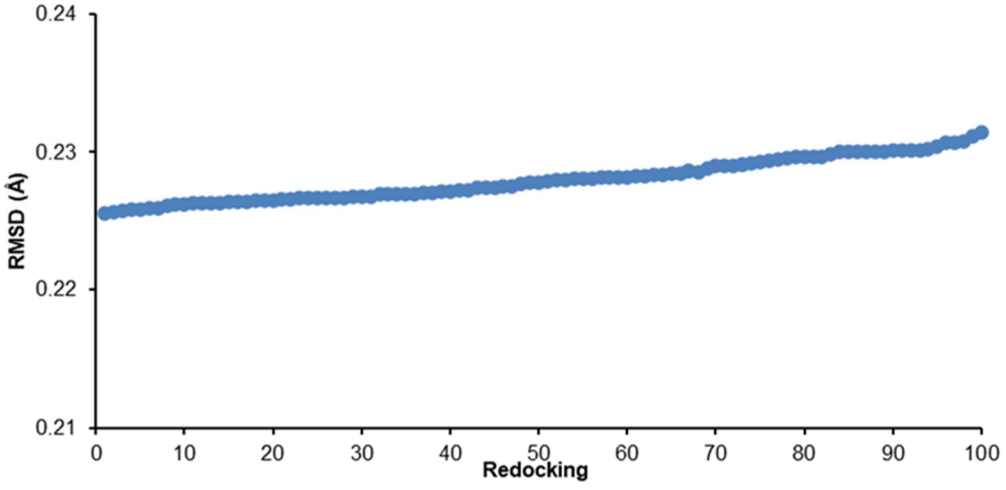

Fig 1. The RMSD values resulting from 100 iterations of redocking

Table 1. Binding energy value and contacting receptor residue from docking result

Ligand	Binding energy (kcal/mol)	Contacting receptor residues
4',6,6',8-Tetrahydroxy-3-methoxyflavon	−6.350	Asp164, Val165, Arg166, Met208, Ala246, Pro247, Pro248, Tyr264, Gly266, Asn267, Tyr268, Gln269, Tyr273, Thr301
3,4',5-Trihydroxy-7,3'-dimethoxyflavon	−6.410	Lys157, Leu162, Gly163, Asp164, Arg166, Glu167, Met208, Ala246, Pro247, Pro248, Tyr264, Tyr 268, Gln269, Tyr273
Taxifolin 3-*O*-α-arabinopyranose	−7.238	Leu162, Gly163, Asp164, Arg166, Glu167, Met208, Ser245, Ala246, Pro247, Pro248, Tyr264, Asn267, Tyr268, Gln 269, Tyr273, Thr301
Quercetin 3-*O*-glucose	−7.299	Asp164, Arg166, Met208, Ser245, Ala246, Pro247, Pro248, Tyr264, Gly266, Asn267, Tyr268, Tyr273, Thr301, Asp302
Quercetin 3-methyl-ether	−7.111	Lys157, Leu162, Gly163, Asp164, Arg166, Glu167, Met208, Ala246, Pro247, Pro248, Tyr264, Tyr268, Gln269, Tyr273, Thr301
Quercetin	−6.847	Asp164, Val165, Arg166, Met208, Pro247, Pro248, Tyr264, Gly266, Asn267, Tyr268, Tyr273, Thr301, Asp302
Taxifolin	−6.614	Asp164, Arg166, Glu167, Met208, Ser245, Ala246, Pro247, Pro248, Tyr264, Gly266, Asn267, Tyr268, Thr301
Quercetin 3'-glucoside	−8.244	Lys157, Leu162, Gly163, Asp164, Arg166, Glu167, Met208, Ala246, Pro247, Pro248, Tyr264, Gly266, Asn267, Tyr268, Gln269, Tyr273, Thr301
5,6-Diepicapsokarpoxanthin	−5.768	Asp164, Arg166, Glu167, Ser170, Tyr171, Gln174, Pro247, Pro248, Tyr264, Gly266, Asn267, Tyr268, Gln269, Tyr273
Capsorubin	−4.470	Asp164, Arg166, Glu167, Ser170, Tyr171, Gln174, Met208, Pro247, Pro248, Tyr264, Gly266, Asn267, Tyr268
Capsanthin 5,6-epoxide	−5.728	Arg166, Glu167, Ser170, Tyr171, Gln174, Met208, Pro247, Pro248, Tyr264, Gly266, Asn267, Tyr268, Gln269
Capsanthin 3,6-epoxide	−5.177	Asp164, Arg166, Glu167, Ser170, Tyr171, Gln174, Pro247, Pro248, Tyr264, Gly266, Asn267, Tyr268, Gln269, Tyr273
Capsanthin	−5.607	Asp164, Arg166, Glu167, Ser170, Tyr171, Gln174, Met208, Pro247, Pro248, Tyr264, Gly266, Asn267, Tyr268, Gln269, Tyr273
Cryptocapsin	−5.683	Asp164, Arg166, Glu167, Ser170, Tyr171, Gln174, Met206, Pro247, Pro248, Tyr264, Gly266, Asn267, Tyr268, Gln269, Tyr273
β-Cryptoxanthin 5,6-epoxide	−4.699	Arg166, Glu167, Ser170, Tyr171, Gln174, Val202, Met208, Pro247, Pro248, Gly266, Asn267, Tyr268
Cryptoxanthin	−4.955	Asp164, Arg166, Glu167, Ser170, Tyr171, Gln174, Met208, Pro247, Pro248, Tyr264, Gly266, Asn267, Tyr268, Gln269
Native ligand	−7.517	Asp164, Arg166, Met208, Pro247, Pro248, Gln250, Tyr264, Thr265, Gly266, Asn267, Tyr268, Gln269, Tyr273, Pro299, Thr301
Remdesivir	−7.442	Lys157, Leu162, Gly163, Asp164, Pro247, Pro248, Tyr264, Thr265, Gly266, Asn267, Tyr268, Gln269, Gly271, Tyr273, Pro299, Thr301
Paxlovid	−7.217	Asp164, Arg166, Glu167, Met208, Ala246, Pro247, Pro248, Tyr264, Gly266, Asn267, Tyr268, Gln269, Tyr273, Pro299, Thr301

This indicates a more robust and stable interaction with the target protein, suggesting its potential as a highly effective ligand (Fig. 2). The low binding energy reflects the ability of quercetin 3'-glucoside to form a significant number of favorable interactions, such as hydrogen bonds and hydrophobic contacts, within the protein's binding site. Consequently, this compound may possess enhanced bioactivity and efficacy, making it a promising candidate for further drug discovery and development investigation.

Fig. 3 illustrates the interactions formed by the compound quercetin 3'-glucoside. The docking results

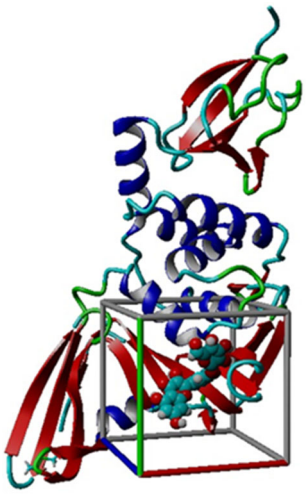

Fig 2. The docking process of quercetin 3'-glucoside

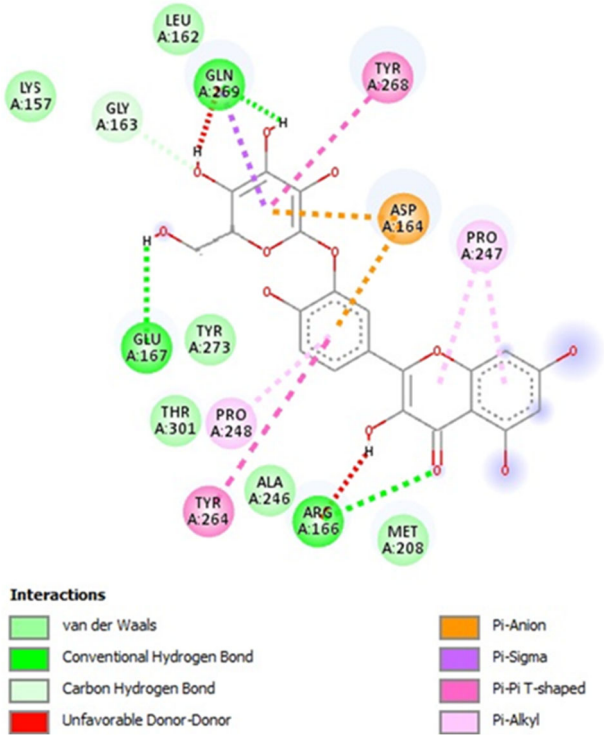

Fig 3. Visualization of ligand-protein complex interactions from molecular docking results

indicate that quercetin 3'-glucoside exhibits strong and specific interactions with the SARS-CoV-2 PLpro protein through various molecular interactions. One of the key interactions is the formation of conventional hydrogen bonds with the amino acid residues of Arg166, Glu167, and Gln269. These hydrogen bonds contribute significantly to the stability of the ligand-protein complex due to their specificity and relatively high interaction energy. This finding suggests that these residues play a crucial role in the binding mechanism of quercetin 3'-glucoside with PLpro.

In addition to hydrogen bonding, hydrophobic interactions also play an essential role in stabilizing the complex. Van der Waals interactions were identified with residues such as Lys157, Leu162, Met208, Ala246, Tyr273, and Thr301, enhancing the binding strength of the compound to the protein. These hydrophobic interactions increase the overall stability of the complex by supporting the surrounding binding site of the protein. Moreover, carbon-hydrogen bonds with the Gly163 residues further contribute to its stability, albeit with less energy compared to conventional hydrogen bonds.

Electronic interactions further enhance ligand-protein binding. Specifically, a pi-anion interaction was observed with Asp164, while pi-sigma and pi-pi T-shaped interactions occurred with Tyr264 and Tyr268, respectively. Additionally, pi-alkyl interactions were identified with Pro247 and Pro248. These electronic contributions not only enhance the binding stability but also provide an additional dimension to the binding mechanism, particularly in terms of the specificity and energy of interaction. The combination of these interactions underscores the ability of quercetin 3'-glucoside to efficiently bind to PLpro.

Although a few unfavorable donor-donor interactions were detected, they do not significantly compromise the overall stability of the ligand-protein complex. Overall, the interaction profile indicates that quercetin 3'-glucoside holds great potential as a SARS-CoV-2 PLpro inhibitor. The stable interactions with key residues such as Arg166, Glu167, and Gln269 further highlight its potential as a promising candidate for antiviral drug development.

MD Simulation

Based on the previous docking stage, quercetin 3'-glucoside emerged as the compound with the most potential in inhibiting SARS-CoV-2 PLpro. MD simulations further deepen the evaluation of the stability of the ligand-protein complex, specifically between quercetin 3'-glucoside and the target protein 7JIR. These

findings reinforce the validity of quercetin 3'-glucoside as a potential candidate in antiviral drug development and pave the way for new opportunities in exploring compound design and optimization for novel drug candidates.

The active site of SARS-CoV-2 PLpro is the region within the enzyme where protein substrate cleavage occurs. This active site contains several key residues crucial for proteolytic catalysis. The primary components of the SARS-CoV-2 PLpro active site include amino acid residues such as Cys111, His272, and Asp286. Beyond the catalytic triad, other residues surrounding the active site play essential roles in substrate stabilization and inhibitor binding. For instance, crystal structures of PLpro bound to inhibitors like GRL-0617 illustrate how inhibitors interact with residues around the active site, including Cys111, His272, Asp286, and additional residues like Gln269, which aid in stabilizing the inhibitor-PLpro complex [32-33].

The visualization of the ligand-protein complex resulting from the MD simulation is shown in Fig. 4. This figure shows hydrogen bonds with the amino acid residues of Tyr268 and Gln269 and other interactions that potentially enhance the inhibitory effect on SARS-CoV-2 PLpro. The detailed examination of Fig. 4 reveals several vital interactions between the ligand and the protein, which are critical for the stabilization and binding affinity of the complex. The hydrogen bonds with Tyr268 and Gln269 play a significant role in forming a stable complex, facilitating the effective inhibition of the target. In addition to these hydrogen bonds, other non-covalent interactions such as van der Waals forces, hydrophobic interactions, and pi-pi stacking further contribute to the ligand-protein complex's overall stability and binding strength. These interactions collectively enhance the binding affinity of the ligand to the SARS-CoV-2 PLpro, making it a potent inhibitor.

Hydrogen bonds and van der Waals interactions significantly influence the binding process. Hydrogen bonds contribute to the stabilization of ligands in protein-ligand interactions, while hydrophobic interactions and van der Waals forces play crucial roles in stabilizing non-polar ligands. Analyzing ligand structures and their binding poses typically aids in understanding these interactions and

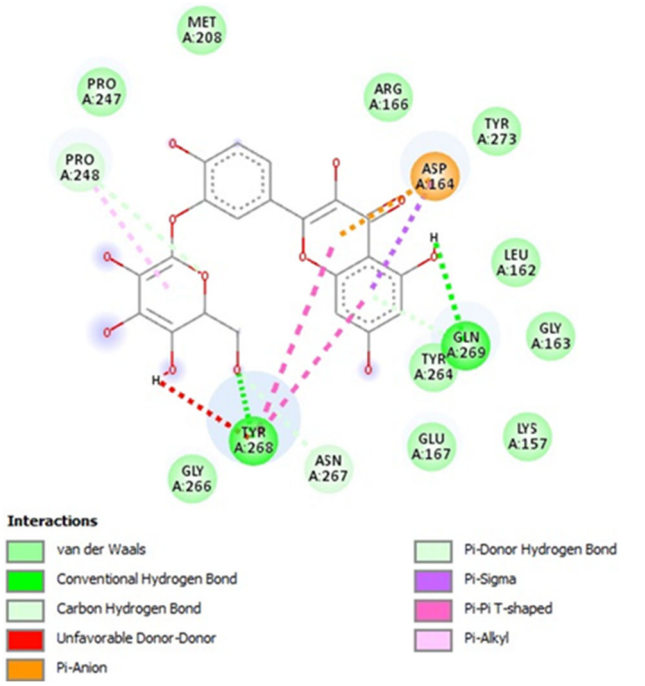

Fig 4. Visualization of ligand-protein complex interactions from MD simulation

determining the binding energy of the compounds [34]. Although van der Waals interactions are generally considered the weakest molecular forces, their cumulative effect can become substantial when multiple van der Waals forces are involved [35].

Interpreting structural changes, particularly differences between two structures is most effectively done through graphical analysis of the RMSD derived from MD simulation trajectories. Smaller RMSD values indicate more significant spatial similarity between the compared structures, while larger RMSD values signify more significant differences. Consequently, higher RMSD values suggest protein system instability. In this context, RMSD analysis is a crucial tool for understanding protein dynamics and conformational changes during simulations. This is important for confirming the simulation model's validity and ensuring the results' reliability for further analysis (Fig. 5).

The RMSD graph derived from the MD simulation provides valuable insight into the structural stability of the system over time. Throughout the 100-ns simulation, the RMSD fluctuates between approximately 2.2 and 2.8 Å, as indicated by the blue line. MD simulation results

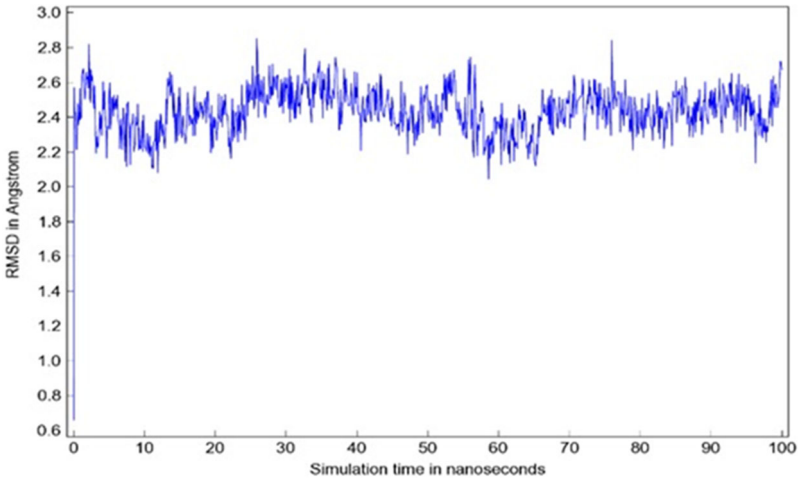

Fig 5. Graph of RMSD vs. time

indicate that after 2 ns, the RMSD values stabilize, suggesting that the protein structure reaches a relatively stable condition after this period. These small fluctuations indicate that the MD simulation has reached stability, with the molecular structure maintaining a consistent conformation. RMSD is a key metric for assessing the structural integrity and conformational changes of a molecule during a simulation, allowing researchers to evaluate its stability over time. The consistent RMSD values observed in this simulation suggest that the structure maintained its overall stability, showing no significant deviations throughout the duration of the analysis. This stability is an important indication of the reliability of the system in further computational studies or potential drug screening.

Additionally, the delta RMSD values calculated at 5 ns intervals reveal that most of these values are below 1 Å, with an average delta RMSD of 0.2702 Å. MD simulations are acceptable if they produce RMSD values below 2 Å [36]. This method serves as a benchmark for assessing structural stability throughout the simulation. After 501 steps, the energy minimization experiment was completed. The system demonstrated a free-binding energy value of −5.9080 kcal/mol, confirming stability in free-binding energy calculations.

Another result from the MD simulation of SARS-CoV-2 PLpro is the root mean square fluctuation (RMSF) values of the amino acid residues, providing insights into the stability of interactions during the simulation period. Each residue's position was measured for its RMSF value, reflecting fluctuations throughout the simulation. Fig. 6 shows the correlation between RMSF values and the number of corresponding residues. These amino acid residue fluctuations occur in response to ligand-induced binding, where increased fluctuation values indicate higher residue flexibility and decreased interaction stability [37]. The study's results suggest that the recommended ligand exhibits high interaction stability within the main catalytic site of SARS-CoV-2 PLpro, as evidenced by the low RMSF values.

The graph presented shows the RMSF values plotted against residue numbers, derived from a MD simulation. On the x-axis, residue numbers range from 0 to 310, while the y-axis represents the RMSF values ranging from 0.75 to 3.75 Å. RMSF is an important measure of the flexibility or movement of each residue in the protein over time. Peaks in the graph indicate residues with greater flexibility, suggesting higher mobility, while troughs represent more stable residues with less movement. This type of analysis is crucial for understanding the dynamic behavior of the protein, as it helps identify regions with significant mobility or structural rigidity. The overall trend observed in this graph shows that while some residues exhibit high fluctuations, the majority of the residues show relatively low and consistent fluctuations. This suggests that, overall, the protein structure remains stable throughout the simulation, with certain regions exhibiting higher mobility. These results from the RMSF

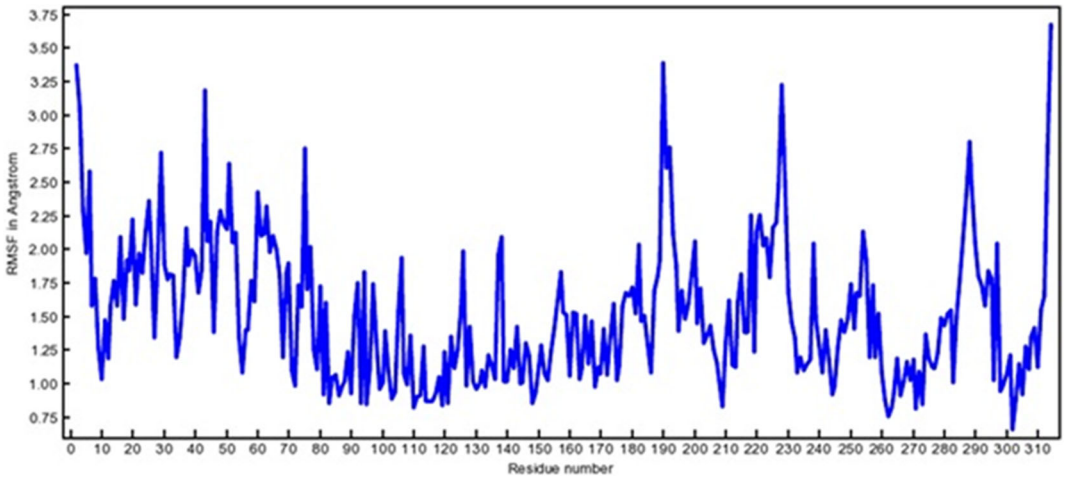

Fig 6. Graph of RMSF vs. residue number

analysis further support the RMSD findings, indicating that the MD simulation has likely reached stability.

■ CONCLUSION

This study highlights the promising potential of Papuan Red Fruit (*Pandanus conoideus* Lam) in combating COVID-19, mainly through inhibiting the SARS-CoV-2 PLpro. Based on docking results conducted on all flavonoid and carotenoid compounds present in the red fruit, quercetin 3'-glucoside was found to have the highest binding energy value of −8.244 kcal/mol. This is supported by hydrogen bonds such as GLN169, which aid in stabilizing the inhibitor PLpro complex. To further confirm the potential of this compound, structural stability was also assessed through MD simulations for 100 ns at a temperature of 300 K. These simulations confirmed that quercetin 3'-glucoside is stable, as indicated by the absence of significant structural changes. Based on these results, quercetin 3'-glucoside shows great potential as an inhibitor of SARS-CoV-2 PLpro.

■ ACKNOWLEDGMENTS

The authors acknowledge the facilities, scientific and technical support from Austrian-Indonesian Center for Computational Chemistry, Department of Chemistry, Faculty of Mathematics and Natural Sciences Universitas Gadjah Mada, Yogyakarta, Indonesia.

■ CONFLICT OF INTEREST

There are no conflicts of interest in this study.

■ AUTHOR CONTRIBUTIONS

Agus Dwi Ananto: Writing–original draft, methodology, investigation, formal analysis, conceptualization; Harno Dwi Pranowo: Writing–review and editing, investigation; Winarto Haryadi and Niko Prasetyo: Writing–review and editing.

■ REFERENCES

[1] Fajriyah, N.N., Mugiyanto, E., Rahmasari, K.S., Nur, A.V., Najihah, V.H., Wihadi, M.N.K., Merzouki, M., Challioui, A., and Vo, T.H., 2023, Indonesia herbal medicine and its active compounds for antidiabetic treatment: A systematic mini review, *Moroccan J. Chem.*, 11 (4), 948–964.

[2] Estiasih, T., Maligan, J.M., Witoyo, J.E., Mu'alim, A.A.H., Ahmadi, K., Mahatmanto, T., and Zubaidah, E., 2025, Indonesian traditional herbal drinks: Diversity, processing, and health benefits, *J. Ethnic Foods*, 12 (1), 7.

[3] Liu, C.X., 2021, Overview on development of ASEAN traditional and herbal medicines, *Chin. Herb. Med.*, 13 (4), 441–450.

[4] Becker, M.M., Nunes, G.S., Ribeiro, D.B., Silva, F.E.P.S., Catanante, G., and Marty, J.L., 2019, Determination of the antioxidant capacity of red fruits by miniaturized spectrophotometry assays, *J. Braz. Chem. Soc.*, 30 (5), 1108–1114.

[5] Purbaya, S., Aisyah, L.S., and Nopitasari, D., 2020, The effectiveness of adding red fruit oil (*Pandanus*

conoideus Lamk.) into ethanol extract of temulawak rhizome (*Curcuma xanthorrhiza* Roxb.) as antioxidant, *J. Kim. Sains Apl.*, 23 (11), 409–413.

[6] Herdiyati, Y., Atmaja, H.E., Satari, M.H., and Kurnia, D., 2024, Potential antibacterial flavonoid from buah merah (*Pandanus conoideus* Lam.) against pathogenic oral bacteria of *Enterococcus faecalis* ATCC 29212, *Open Dent. J.*, 14, 433–439.

[7] Achadiani, A., Sastramihardja, H., Akbar, I.B., Hernowo, B.S., Faried, A., and Kuwano, H., 2013, Buah merah (*Pandanus conoideus* Lam.) from Indonesian herbal medicine induced apoptosis on human cervical cancer cell lines, *Obes. Res. Clin. Pract.*, 7 (Suppl. 1), 31–32.

[8] Anggadiredja, K., Lestari, I.T., Garmana, A.N., and Utami, R.A., 2025, Anti diabetic peripheral neuropathy of red fruit (*Pandanus conoides* Lamk) oil in a rat model: Involvement of oxidative and neuroinflammatory pathways, *Int. J. Neuropsychopharmacol.*, 28 (Suppl. 1), i237–i238.

[9] Tambaip, T., Br Karo, M., Hatta, M., Dwiyanti, R., Natzir, R., Massi, M.N., Asadul Islam, A., and Djawad, K., 2018, Immunomodulatory effect of orally red fruit (*Pandanus conoideus*) extract on the expression of CC chemokine receptor 5 mRNA in HIV patients with antiretroviral therapy, *Res. J. Immunol.*, 11 (1), 15–21.

[10] Tambunan, I.W., Gunawan, E., and Pratiwi, R.D., 2023, Antibacterial activity test of yoghurt paste red fruit (*Pandanus conoideus* Lam.) against *Escherichia coli*, *J. Pharmacol. Res. Dev.*, 5 (1), 19–27.

[11] World Health Organization, 2024, *COVID-19 Epidemiological Update – 15 March 2024*, https://www.who.int/publications/m/item/covid-19-epidemiological-update-15-march-2024.

[12] Kandeel, M., Abdelrahman, A.H.M., Oh-Hashi, K., Ibrahim, A., Venugopala, K.N., Morsy, M.A., and Ibrahim, M.A.A., 2021, Repurposing of FDA-approved antivirals, antibiotics, anthelmintics, antioxidants, and cell protectives against SARS-CoV-2 papain-like protease, *J. Biomol. Struct. Dyn.*, 39 (14), 5129–5136.

[13] Pang, J., Gao, S., Sun, Z., and Yang, G., 2021, Discovery of small molecule PLpro inhibitor against COVID-19 using structure-based virtual screening, molecular dynamics simulation, and molecular mechanics/generalized born surface area (MM/GBSA) calculation, *Struct. Chem.*, 32 (2), 879–886.

[14] Rizzuti, B., Grande, F., Conforti, F., Jimenez-Alesanco, A., Ceballos-Laita, L., Ortega-Alarcon, D., Vega, S., Reyburn, H.T., Abian, O., and Velazquez-Campoy, A., 2021, Rutin is a low micromolar inhibitor of SARS-CoV-2 main protease 3CLpro: Implications for drug design of quercetin analogs, *Biomedicines*, 9 (4), 375.

[15] Kashyap, P., Thakur, M., Singh, N., Shikha, D., Kumar, S., Baniwal, P., Yadav, Y.S., Sharma, M., Sridhar, K., and Inbaraj, B.S., 2022, *In silico* evaluation of natural flavonoids as a potential inhibitor of coronavirus disease, *Molecules*, 27 (19), 6374.

[16] Pinzi, L., and Rastelli, G., 2019, Molecular docking: Shifting paradigms in drug discovery, *Int. J. Mol. Sci.*, 20 (18), 4331.

[17] Rahman, M.M., Islam, M.R., Akash, S., Mim, S.A., Rahaman, M.S., Emran, T.B., Akkol, E.K., Sharma, R., Alhumaydhi, F.A., Sweilam, S.H., Hossain, M.E., Ray, T.K., Sultana, S., Ahmed, M., Sobarzo-Sánchez, E., and Wilairatana, P., 2022, *In silico* investigation and potential therapeutic approaches of natural products for COVID-19: Computer-aided drug design perspective, *Front. Cell. Infect. Microbiol.*, 12, 929430.

[18] Masone, D., and Grosdidier, S., 2014, Collective variable driven molecular dynamics to improve protein–protein docking scoring, *Comput. Biol. Chem.*, 49, 1–6.

[19] Childers, M.C., and Daggett, V., 2017, Insights from molecular dynamics simulations for computational protein design, *Mol. Syst. Des. Eng.*, 2 (1), 9–33.

[20] Krieger, E., Koraimann, G., and Vriend, G., 2002, Increasing the precision of comparative models with YASARA NOVA–A self-parameterizing force field, *Proteins: Struct., Funct., Bioinf.*, 47 (3), 393–402.

[21] BIOVIA, Dassault Systèmes, 2020, *Discovery Studio Visualizer ver. 21.1.0.20298*, Dassault Systèmes, San Diego, US.

[22] Osipiuk, J., Azizi, S.A., Dvorkin, S., Endres, M., Jedrzejczak, R., Jones, K.A., Kang, S., Kathayat, R.S., Kim, Y., Lisnyak, V.G., Maki, S.L., Nicolaescu, V., Taylor, C.A., Tesar, C., Zhang, Y.A., Zhou, Z., Randall, G., Michalska, K., Snyder, S.A., Dickinson, B.C., and Joachimiak, A., 2021, Structure of papain-like protease from SARS-CoV-2 and its complexes with non-covalent inhibitors, *Nat. Commun.*, 12 (1), 743.

[23] Suprijono, M.M., Widjanarko, S.B., Sujuti, H., and Kurnia, D., 2019, Computational study of antioxidant activity and bioavailability of papua red fruit (*Pandanus conoideus* Lam.) flavonoids through docking toward human serum albumin, *AIP Conf. Proc.*, 2108 (1), 020020.

[24] Heriyanto, H., Gunawan, I.A., Fujii, R., Maoka, T., Shioi, Y., Kameubun, K.M.B., Limantara, L., and Brotosudarmo, T.H.P., 2021, Carotenoid composition in buah merah (*Pandanus conoideus* Lam.), an indigenous red fruit of the Papua Islands, *J. Food Compos. Anal.*, 96, 103722.

[25] Nugraha, G., and Istyastono, E.P., 2021, Virtual target construction for structure-based screening in the discovery of histamine H_2 receptor ligands, *Int. J. Appl. Pharm.*, 13 (3), 239–241.

[26] Nugraha, G., Pranowo, H.D., Mudasir, M., and Istyastono, E.P., 2022, Virtual target construction for discovery of human histamine H4 receptor ligands employing a structure-based virtual screening approach, *Int. J. Appl. Pharm.*, 14 (4), 213–218.

[27] Lengauer, T., and Rarey, M., 1996, Computational methods for biomolecular docking, *Curr. Opin. Struct. Biol.*, 6 (3), 402–406.

[28] Nurhidayah, M., Fadilah, F., Arsianti, A., and Bahtiar, A., 2022, Identification of FGFR inhibitor as ST2 receptor/interleukin-1 receptor-like 1 inhibitor in chronic obstructive pulmonary disease due to exposure to E-cigarettes by network pharmacology and a molecular docking prediction, *Int. J. Appl. Pharm*, 14 (2), 256–266.

[29] Stasiulewicz, A., Maksymiuk, A.W., Nguyen, M.L., Bełza, B., and Sulkowska, J.I., 2021, SARS-CoV-2 papain-like protease potential inhibitors—*In silico* quantitative assessment, *Int. J. Mol. Sci.*, 22 (8), 3957.

[30] Kleem, T., Ebert, G., Calleja, D.J., Allison, C.C., Richardson, L.W., Bernardini, J.P., Lu, B.G.C., Kuchel, N.W., Grohmann, C., Shibata, Y., Gan, Z.Y., Cooney, J.P., Doerflinger, M., Au, A.E., Blackmore, T.R., van der Heden van Noort, G.J., Geurink, P.P., Ovaa, H., Newman, J., Riboldi-Tunnicliffe, A., Czabotar, P.E., Mitchell, J.P., Feltham, R., Lechtenberg, B.C., Lowes, K.N., Dewson, G., Pellegrini, M., Lessene, G., and Komander, D., 2020, Mechanism and inhibition of the papain-like protease, PLpro, of SARS-CoV-2, *EMBO J.*, 39 (18), e106275.

[31] Ananto, A.D., Pranowo, H.D., Haryadi, W., and Prasetyo, N., 2024, Flavonoid compound of red fruit Papua and its derivatives against SARS-CoV-2 Mpro: An *in silico* approach. *J. Appl. Pharm. Sci.*, 14 (12), 90–97.

[32] Calleja, D.J., Lessene, G., and Komander, D., 2022, Inhibitors of SARS-CoV-2 PLpro, *Front. Chem.*, 10, 876212.

[33] Gao, X., Qin, B., Chen, P., Zhu, K., Hou, P., Wojdyla, J.A., Wang, M., and Cui, S., 2020, Crystal structure of SARS-CoV-2 papain-like protease, *Acta Pharm. Sin. B*, 11 (1), 237–245.

[34] Meng, X.Y., Zhang, H.X., Mezei, M., and Cui, M., 2011, Molecular docking: A powerful approach for structure-based drug discovery, *Curr. Comput.-Aided Drug Des.*, 7 (2), 146–157.

[35] Barratt, E., Bingham, R.J., Warner, D.J., Laughton, C.A., Phillips, S.E.V., and Homans, S.W., 2005, Van der Waals interactions dominate ligand protein association in a protein binding site occluded from solvent water, *J. Am. Chem. Soc.*, 127 (33), 11827–11834.

[36] Zhang, Q.Y., and Aires-de-Sousa, J., 2007, Random forest prediction of mutagenicity from empirical physicochemical descriptors, *J. Chem. Inf. Model.*, 47 (1), 1–8.

[37] Chaudhary, N., and Aparoy, P., 2017, Deciphering the mechanism behind the varied binding activities of COXIBs through Molecular Dynamic Simulations, MM-PBSA binding energy calculations and per-residue energy decomposition studies, *J. Biomol. Struct. Dyn.*, 35 (4), 868–882.